

1 **1 Point-by-point response**

2 **1.1 Referee 1**

3 For the point-by-point response, please see [https://www.nat-hazards-earth-syst-sci-discuss.net/nhess-](https://www.nat-hazards-earth-syst-sci-discuss.net/nhess-2019-8/nhess-2019-8-AC1-supplement.pdf)
4 2019-8/nhess-2019-8-AC1-supplement.pdf.

5 **1.2 Referee 2**

6 For the point-by-point response, please see [https://www.nat-hazards-earth-syst-sci-discuss.net/nhess-](https://www.nat-hazards-earth-syst-sci-discuss.net/nhess-2019-8/nhess-2019-8-AC2-supplement.pdf)
7 2019-8/nhess-2019-8-AC2-supplement.pdf.

8 **1.3 Editor**

9 We thank you for your comments that will help us improve our manuscript. Here we reply point-by-point
10 to the issues raised by the Editor. Our answers are highlighted in green colour.

11 (1) English has to be strongly revised with the help of some native English-speaker.

12 **We have proof read the paper carefully and revised the grammar errors in this revision.**

13 (2) The structure of the work must be improved according to the suggestions of Referee #2. Carefully
14 separate Introduction from area description, methods, results and discussion of results in separate and
15 self-contained sections.

16 **Thanks. The structure of this manuscript has been reorganised.**

17 (3) Modify the writing and the approach so as to support each statement with proofs and/or references to
18 published papers.

19 **In the revised manuscript, we checked and rephrased the related sentences.**

20 (4) Greatly improve the references to previous work of similar type (most of the widely known work on
21 landslide susceptibility is not cited).

22 **According to your suggestions, some descriptions and references were added in the revised manuscript.**

23 (5) Please try to modify the approach of the study to highlight the relevance to a susceptibility study which
24 deals with the specific problem of an M7 trigger, as also underlined by referee #2.

25 **In this revision, we modified some sentences related to the approach.**

26 (6) Please add a reference to tables and figures in the text, when needed.

27 **Thanks for your kind reminding. We checked and revised the related sentences.**

28 (7) Please improve and enlarge the methodology section, by providing more details on the procedure and
29 on the methods used.

1 According to your and referee's suggestions, we reorganised the methodology section of the study. The
2 flowchart was added in the revised manuscript. Now, we think it's clear and easy to understand.

3 (8) Please also revise and answer to each minor comment provided by the referees as well.

4 Thanks for your kind reminding. We have read each comment carefully. In this revision, we have made
5 substantial improvements to the paper according to each comment. We rephrased each sentence
6 mentioned in the referees' comments and improved the writing of the whole article carefully.

7 **2 List of relevant changes**

8 We have:

- 9 (1) reorganised the structure of the manuscript,
- 10 (2) improved the writing of the whole article,
- 11 (3) more clearly stated the objectives and framework,
- 12 (4) completely reorganised and expanded the methodology section,
- 13 (5) modified and deleted some useless sentences as suggested,
- 14 (6) improved the quality of the figures as suggested,
- 15 (7) added some references as suggested,
- 16 (8) revised the results and improved the discussions.

17

GIS-based earthquake-triggered landslide susceptibility mapping with an integrated weighted index model in Jiuzhaigou region of Sichuan Province, China

Yaning Yi ^{1,2}, Zhijie Zhang ^{3,*}, Wanchang Zhang ^{1,*}, Qi Xu ⁴, Cai Deng ¹ and Qilun Li ^{1,2}

¹Key Laboratory of Digital Earth Science, Institute of Remote Sensing and Digital Earth, Chinese Academy of Sciences, Beijing 100094, China

²University of Chinese Academy of Sciences, Beijing, 100049, China

³Department of Geography, University of Connecticut, Storrs, CT, 06269, USA

⁴Institute of Karst Geology, Chinese Academy of Geological Sciences, Guilin 541004, China

Correspondence to: Zhijie Zhang (zhijie.zhang@uconn.edu) and Wanchang Zhang (zhangwc@radi.ac.cn)

Abstract. A ~~Ms 7.0~~ Mw 6.5 earthquake struck the Jiuzhaigou region of Sichuan Province, China at 21:19 pm on Tuesday, 8 August 2017, ~~which and~~ triggered a large number of landslides. For mitigating the damages of earthquake-triggered landslides to individuals and infrastructures of the earthquake affected region, a comprehensive landslide susceptibility mapping was attempted with an integrated weighted index model by combining the frequency ratio and the analytical hierarchy process approaches under GIS-based environment in the earthquake heavily attacked Zhangzha town of the Jiuzhaigou region. For this purpose, a total number of 842 earthquake-triggered landslides were visually interpreted and located from Sentinel-2A images acquired before and after the earthquake at first, and then the recognized landslides were randomly split into two groups to establish the earthquake-triggered landslide inventory, among which 80 % of the landslides was used for training the integrated model and the remaining 20 % for validation. ~~Nine landslide controlling factors, namely slope, aspect, elevation, lithology, distance from faults, distance from rivers, land use/cover, normalized difference vegetation index and peak ground acceleration, were considered with an integrated weighted index model for determination of the weighted index through analysing their relationships with occurrence frequency ratios of landslides with analytical hierarchy process approaches.~~ Nine landslide controlling factors were considered including slope, aspect, elevation, lithology, distance from faults, distance from rivers, land-use/cover, normalized difference vegetation index and peak ground acceleration. The frequency ratio was utilized to evaluate the contribution of each landslide controlling factor on landslide occurrence, and the analytical hierarchy process was used to analysis the mutual relationship between landslide controlling factors. Finally, the landslide susceptibility map was produced by using the weighted overlay analysis. Furthermore, an area under the curve approach was adopted to comprehensively evaluate the performance of the integrated weighted index model, including the degree of model fit and model predictive capability. The results demonstrated the reliability and feasibility of the integrated weighted index model in earthquake-triggered landslide susceptibility mapping at regional scale. The generated map can ~~be served as the scientific basis~~

1 ~~to~~ help engineers and decision makers assess and mitigate hazards of the earthquake-triggered landslides to individuals and
2 infrastructures of the earthquake affected region.

3

4 **Keywords**

5 Earthquake-triggered landslide susceptibility mapping; An integrated weighted index model; Frequency ratio; Analytical
6 hierarchy process; The Jiuzhaigou region

7

8 **1 Introduction**

9 Recent natural disasters and their associated death tolls and financial costs have put mitigation of natural hazards at the
10 forefront of societal needs. Landslides are the most common natural disasters (geological hazards) that cause ~~damages to~~
11 ~~people's lives and property~~ heavy human casualties and damage to property every year in many areas of the world (Saha et al.,
12 2010; Su et al., 2015). ~~Landslides are more likely to occur when the slope becomes unstable. Slope instability can be caused~~
13 ~~by several factors, such as geological, meteorological and anthropogenic factors, especially the earthquake and rainfall~~
14 Landslides can be caused by several factors, such as strong earthquakes, intense or prolonged rainfall and multiple human
15 actions (Guzzetti et al., 2012; Sato et al., 2007).

16 On August 8, 2017, a catastrophic earthquake of magnitude ~~7.0~~ 6.5 struck the Jiuzhaigou region of Sichuan Province, China.
17 The epicentre of this earthquake with a depth of 20 km was located latitude 33.20° N and longitude 103.82° E close to the
18 Jiuzhaigou National Nature Reserve, about 39 km West ~~from~~ to the city of Jiuzhaigou. According to China Earthquake
19 Administration, ~~the epicentre of the Jiuzhaigou earthquake was located near the Minjiang, Tazang and Huya faults (as can be~~
20 ~~seen in Fig. 1), and~~ this earthquake was caused by tectonic movement of an NW-SE-oriented left-lateral strike-slip fault (Wang
21 et al., 2018a). Although the intense rainfall was not observed after the earthquake, numerous landslides were triggered yet by
22 strong seismic vibration of ground (Zhao et al., 2018). ~~Many tourists were trapped in the region due to numerous landslides~~
23 ~~blocking the roads.~~ Many scenic spots in the Jiuzhaigou National Nature Reserve were destroyed, as presented in Fig. 2(b),
24 the Sparkling Lake was damaged. Due to numerous landslides blocking the roads, many tourists were trapped in the region, as
25 can be seen in Fig. 2(d), the S301 highway was severely obstructed by a significant number of small-scale landslides. Based
26 on field investigation, most of these landslides were small-scale rock slides, rock falls and debris slides (Fan et al., 2018; Zhao
27 et al., 2018). As China Earthquake Administration reported, this earthquake caused 25 deaths and 176,492 injured or affected
28 (Lei et al., 2018; Wang et al., 2018b). Landslides seriously threaten the anthropogenic activities, as well as tourist facilities of

1 [the region](#). Comprehensive earthquake-triggered landslide susceptibility mapping in the earthquake affected area, therefore, is
2 essential to [assess landslide hazard and](#) mitigate landslide damages through the proper prevention actions for the future.

3 Over the last decades, many approaches for landslide susceptibility mapping were proposed, among which the application of
4 remote sensing associated with GIS modelling techniques became the most popular and effective ones (Alexander, 2008;
5 Carrara et al., 1991; Dai and Lee, 2002; Guzzetti et al., 1999; Lee, 2005; Mantovani et al., 1996; Mansouri Daneshvar, 2014;
6 Xu et al., 2012a). The most commonly used methods for landslide susceptibility mapping include logistic regression (Ayalew
7 and Yamagishi, 2005; Bai et al., 2010; [Manzo et al., 2013](#); Ozdemir and Altural, 2013), weights of evidence (Althuwaynee et
8 al., 2012; Regmi et al., 2010), analytical hierarchy process (AHP) (Kayastha et al., 2013; Komac, 2006; Mansouri Daneshvar,
9 2014; Yalcin, 2008), frequency ratio (FR) (Guo et al., 2015; [Lee and Pradhan, 2007](#); Li et al., 2017; Mohammady et al., 2012),
10 support vector machine (SVM) (Marjanović et al., 2011; Su et al., 2015), decision tree (Nefeslioglu et al., 2010; Saito et al.,
11 2009) and artificial neural network (ANN) ([Caniani et al., 2008](#); [Catani et al., 2005](#); Conforti et al., 2014; [Ermini et al., 2005](#);
12 [Pradhan and Lee, 2009](#)). These methods have been proved capable of mapping the locations that are prone to landslides,
13 however, some shortcomings yet exist in these methods, which reduce the efficiency of these susceptibility methods when
14 applied individually (Tien Bui et al., 2012; Umar et al., 2014). For example, the AHP can be used to identify the mutual
15 relationship between landslide controlling factors and the landslide susceptibility, but the process and results mostly depend
16 on the expert's knowledge, which are somehow subjective in practice (Youssef et al., 2015; Zhang et al., 2016). The FR is
17 capable of representing the influence of the categories of each controlling factor due to landslide occurrences (Lee and Talib,
18 2005), however, the mutual relationship between the factors is mostly neglected ([Zhang et al., 2016](#)), and the same issue also
19 exists in the modelled result. Logistic regression is good at analysing the relationships among the landslide controlling factors
20 but is not capable to evaluate the impact of the categories of each factor individually on landslides (Umar et al., 2014). Fuzzy
21 logic has also been employed in landslide susceptibility mapping, but the modelled results largely rely on the expert's
22 knowledge, which often leads to a high degree of uncertainty (Tilmant et al., 2002). In addition, machine learning models (e.g.
23 SVM, decision tree and ANN models) are very popular methods in landslide analysis, nevertheless, heavy dependence of a
24 very high-speed computer along with large amounts of training data needed constrain their practical applications to some
25 extent (Umar et al., 2014).

26 In addition, the combined approach has been gradually used for landslide susceptibility assessment (Ba et al., 2017; Boon et
27 al., 2015; Dehnavi et al., 2015; Kadavi et al., 2018; Pham et al., 2018; Shrestha et al., 2017; Umar et al., 2014; Youssef et al.,
28 2015). For instance, Umar et al. (~~Umar et al., 2014~~) used an ensemble method of FR and logistic regression to assess the
29 landslide susceptibility in West Sumatera Province, Indonesia, and the similar integrated method was also applied by Youssef
30 et al. (~~Youssef et al., 2015~~). Dehnavi et al. (~~Dehnavi et al., 2015~~) combined the step-wise weight assessment ratio analysis

1 method and adaptive neuro-fuzzy inference system to produce a landslide susceptibility map of Iran. Ba et al. (Ba et al., 2017)
2 proposed an improved information value model based on grey clustering for landslide susceptibility mapping in Chongqing.
3 Kadavi et al. (Kadavi et al., 2018) proposed a hybrid machine learning approach of AdaBoost, LogitBoost, Multiclass Classifier,
4 and Bagging models for spatial prediction of landslides. Although those studies suggested effectiveness of the integrated
5 method in some areas of the world, the universality and efficiency of the integrated method were yet remained as an important
6 issue to be confirmed in different regions of the world (Reichenbach et al., 2018).

7 The main purpose of this study ~~was to apply an integrated weighted index model by combining FR and AHP for susceptibility~~
8 ~~mapping of earthquake triggered landslides.~~ is to map the susceptibility of earthquake-triggered landslides by applying an
9 integrated weighted index model by combining FR and AHP. The integrated model is capable of evaluating the contribution
10 of each landslide controlling factor to landslide occurrence using FR method, meanwhile taking mutual relationships among
11 controlling factors into account by the use of AHP. Such integration is capable to generate a complete model that largely
12 restrains the shortcomings of these two individual methods and reduces the uncertainty and subjectivity resulted by the
13 utilization of individual method. The experiment site was selected at the Zhangzha town of Jiuzhaigou, a region seriously
14 affected by the Jiuzhaigou earthquake. An earthquake-triggered landslide susceptibility map was produced by using the
15 integrated weighted index model along with the remotely sensed information, and a detailed validation analysis by using an
16 area under the curve approach was conducted to the generated susceptibility map of the study area for evaluating the reliability
17 and feasibility of the integrated model. This manuscript is structured as follows: Section 2 introduces the study area ~~and the~~
18 ~~basic information about the earthquake happened on August 8, 2017.~~ Section 3 describes the data utilized and data preparing
19 procedures. Section 4 gives the detailed explanation about the integrated weighted index model. Section 5 presents the results
20 and discussions focusing on validations on the generated earthquake-triggered landslide susceptibility map of the study area
21 followed by the conclusions drawn in Section 6 at the end.

22 2 Study area

23 The study area with an area of about 1345.19 km², as shown in Fig. 1, is located in the Zhangzha town of Jiuzhaigou County
24 between 33.03° N – 33.35° N Latitude and 103.63° E – 104.05° E Longitude in the Min Shan Mountains ~~to~~ to the north of the
25 Sichuan basin, eastern margin of the Tibetan Plateau. As pointed out in Deng (2011), the geological conditions of this region
26 are extremely complex, and the tectonic movement strongly uplifted the entire western region of Jiuzhaigou, while the eastern
27 region had different fault block movements along the early faults. Regional tectonic movements are intense (Wang et al.,
28 2018b), as summarized in Fan et al. (2018), more than 50 earthquake events with magnitude 5.0 or greater occurred in the
29 Jiuzhaigou area in the past century. Active regional tectonic uplift and tilting cause the elevation of the study area to vary from

1 1624 m to 4855 m above mean sea level. ~~The soluble carbonate rocks are widely distributed along with tufa deposition of karst~~
2 ~~developed, and regional tectonic movements are intense here (Wang et al., 2018b). The topography of the region is~~
3 ~~characterized by alpine karst terrain where the elevation varies from 1624 m to 4855 m above mean sea level.~~ The Jiuzhaigou
4 County belongs to a cold sub-humid and cold semi-arid monsoon climate with the annual precipitation about 550 mm (Li et
5 al., 2014). ~~The geomorphology of the study area is jointly formed by the climatic, geotectonic, lithological conditions under~~
6 ~~the effect of topography of the region.~~ The topography of the region is characterized by alpine karst terrain formed by glacial,
7 hydrological and tectonic activity, and with karstification in travertine deposits, many travertine dikes and shoals appeared in
8 the study area. Soluble carbonate rocks are widely distributed along with tufa deposition of karst developed. Due to abundant
9 recharge supply of groundwater in this region, many lakes and streams develop over extensive alpine karst developed region,
10 which favours the hill slope erosion processes, and results in frequent occurrence of rock slides, debris flows, and rock falls
11 there (Florsheim et al., 2013).

12 ~~The Jiuzhaigou National Nature Reserve, approved as the UNESCO World Biosphere Reserve, is just located in the study area.~~
13 ~~Many scenic spots in the Jiuzhaigou National Nature Reserve were destroyed in 2017 by the Jiuzhaigou earthquake, as~~
14 ~~presented in Fig. 2(b), the Sparkling Lake was damaged. A significant number of small scale landslides, as shown in Fig. 1,~~
15 ~~were triggered by this earthquake along roads and river valley where many residents and infrastructures are located. Landslides~~
16 ~~seriously threaten the anthropogenic activities, as well as tourist facilities of the region, as can be seen in Fig. 2(d), the S301~~
17 ~~highway was severely obstructed by rock falls and rock slides, which drawn great attentions extensively.~~

18 3 Data

19 In order to map the landslide susceptibility of the study area, we designed and developed a spatial database with the help of
20 ArcGIS (version 10.2) software. This database contained two primary parts: (1) the landslide inventory dataset for earthquake-
21 triggered landslides; and (2) the datasets of background condition representing the landslide controlling factors. The data layers
22 used in the landslide susceptibility mapping were briefly described ~~as presented in the~~ Table 1.

23 3.1 Landslide inventory

24 Landslide inventory is essential for ~~analysing the relationships between controlling factors and the landslide occurrences, and~~
25 ~~also useful for~~ assessing landslide hazard or risk on a regional scale (Pellicani and Spilotro, 2015). The Jiuzhaigou earthquake
26 ~~on August 8, 2017 with a magnitude of 7.0~~ triggered numerous landslides in the study area. ~~For deriving~~ To derive landslide
27 inventory containing detailed and reliable information on landslide distribution, location, etc., Sentinel-2A images ~~acquired~~ on
28 July 29, August 13 and September 7, 2017 were used to recognize and locate the earthquake-triggered landslides. Sentinel-2A
29 image has 13 spectral bands (from ~~the~~ blue to ~~the~~ shortwave infrared) with the spatial resolution of 10 m, 20 m and 60 m,

1 respectively. In this study, three visible bands (red, green, blue) with the spatial resolution of 10 m were adopted to ~~establish~~
2 ~~the image feature sets of earthquake-triggered landslides based on the visual interpretation of the landslide image~~
3 ~~characteristics.~~ analysis the image characteristics of earthquake-triggered landslides. With the aid of ~~computer and GIS tools~~
4 ~~ArcGIS and ENVI tools~~, the landslide information of the study area was extracted using on-screen visual interpretation on pre-
5 and post-earthquake Sentinel-2A images, ~~as examples presented in Fig. 2.~~ In order to ensure the quality of visual interpretation,
6 GF-1 images with spatial resolution of 2 m ~~acquired~~ on January 15, 2017, were used to verify the results. Consequently, a total
7 number of 842 earthquake-triggered landslides were recognized and positioned. Smaller landslides ~~with total pixels less than~~
8 ~~20~~ were not included as they were not clear enough in visual features. We assumed that the distribution of the earthquake-
9 triggered landslides was reasonably accurate and complete at regional scale in order to make the problem tractable. For
10 earthquake-triggered landslide susceptibility mapping, the landslide inventory dataset was randomly split into two groups,
11 among which 80 % (673 landslides) of the recognized landslides was used for training the integrated weighted index model
12 and the remaining 20 % (169 landslides) for validation.

13 3.2 Landslide controlling factors

14 The occurrence of landslides is a consequence of geological, meteorological, anthropogenic and triggering factors, commonly
15 referred to as landslide controlling factors (Bai et al., 2010). Standard guidelines for choosing the optimal landslide controlling
16 factors are unavailable, but the scale of ~~the~~ analysis, the nature of the study area, the data availability and the quasi-empirical
17 and statistical criteria in literatures can be referenced (Romer and Ferentinou, 2016; Zhou et al., 2016). In ~~present~~ this study,
18 slope, aspect, elevation, lithology, distance from faults, distance from rivers, land-use/cover (LULC), normalized difference
19 vegetation index (NDVI) and peak ground acceleration (PGA) were selected as the landslide controlling factors, as shown in
20 Fig. 3, ~~for analysis.~~

21 Among all landslide controlling factors, slope, aspect and elevation have been recognized as the most important topographic
22 factors closely related to landslides (Ayalew and Yamagishi, 2005; Chalkias et al., 2016). Slope directly affects the velocity
23 of both surface and subsurface flows (Su et al., 2015). ~~Pioneer studies suggested that Landslides~~ become ~~more~~ possible once
24 the slope gradient is higher than 15° (Lee and Min, 2001). In the study area, the slopes were generally steep, with an average
25 slope angle of about ~~29.92~~ 30°. Aspect, referred to the direction of slope faces, is related to ~~the~~ soil moisture, surface runoff
26 and vegetation ~~growing conditions~~, which indirectly affects ~~the~~ landslide development (Zhang et al., 2016). The elevation, as
27 the measure of the land surface height, is a key factor determining gravitational potential energy of terrain and ~~was~~ ~~is~~ often
28 considered in relevant studies (Conforti et al., 2014; Peng et al., 2014). ~~In the study area, the rugged terrain makes the slope~~
29 ~~very unstable.~~ Topographic factors can be calculated with DEM. The DEM from SRTM database was used to extract slope
30 (0°–78°), aspect and elevation (1624--4855 m ~~in the study area~~) in the study area.

1 Lithology is directly related to the slope stability, which plays an important role as one of landslide controlling factors (Guo
2 et al., 2015, Saha et al., 2002). Ten geological formation units including Quaternary (Q, Qh), Triassic (T1, T2, T3), Permian
3 (P, P2), Carboniferous (C), and Devonian (D) outcrop in the study area (Wang et al., 2018a). ~~For~~ During the Jiuzhaigou
4 earthquake, most landslides in the study area occurred in the carboniferous formations which is mainly composed of
5 metamorphic quartzite sandstones, limestone and slate (Fan et al., 2018). In addition, the Permian limestone and Triassic
6 sandstone also exhibited a large number of landslides. In this study, the lithological data was obtained from the geological map
7 at 1: 500,000 scale and was digitized in ArcGIS for further analysis. The distances of a slope from faults as well as from the
8 river channels are also important factors in terms of slope stability (Kanungo et al., 2006). In addition, earthquake-triggered
9 landslides usually are usually found in the vicinity of active faults. Hence, the distances of a slope from geological tectonic
10 zone were often taken into account in slope stability analysis. ~~According to the China Earthquake Administration, the epicentre~~
11 ~~of the Jiuzhaigou earthquake was located near the Minjiang, Tazang and Huya faults. Some studies~~ Fan et al. (2018) had
12 revealed that this earthquake occurred along a previously unknown blind fault probably belonging to a south branch of the
13 Tazang fault or north part of the Huya fault (~~Fan et al., 2018~~). However, due to its great uncertainty, this blind fault was not
14 taken into account in the study area. In this study, the faults were digitized from the geological map at 1: 500,000 scale, and
15 the river channels were interpreted from remote sensing images. ~~Streams also have an impact on the slope stability because~~
16 ~~soil water erosion is prone to take place next to the rivers on slopes.~~ And the LULC map is one of controlling factors that pose
17 direct impact on the occurrence of landslides (Song et al., 2012; Mansouri Daneshvar, 2014). ~~For the Jiuzhaigou earthquake,~~
18 ~~most landslides in the study area occurred in the wood land.~~ In this study, ~~the lithological data was obtained from the geological~~
19 ~~map at 1: 500,000 scale and was digitized in ArcGIS for further analysis.~~ the LULC map was downloaded from the
20 Geographical Information Monitoring Cloud Platform.

21 Vegetation coverage poses effect on soil water erosion, which indirectly affects the occurrence of landslides. NDVI, as the
22 measure of vegetation coverage, ~~was~~ is usually adopted in landslide susceptibility analysis (Siqueira et al., 2015). The NDVI
23 ~~was~~ is calculated from these individual measurements as follows:

$$24 \quad NDVI = \frac{DN_{NIR} - DN_R}{DN_{NIR} + DN_R}, \quad (1)$$

25 Where, DN_{NIR} stands for the spectral reflectance derived from the measured radiances in the near-infrared regions (NIR), and
26 DN_R stands for the spectral reflectance derived from the measured radiances in the visible (Red) regions.

27 In this study, the NDVI map was generated from the Landsat-8 image acquired on April 8, 2017 over the study area.

28 ~~As an important dynamic factor, earthquake~~ Earthquake as an important dynamic factor, often triggers slope failures (Xu et
29 al., 2012a). Usually, the impact of earthquake on landslides ~~was~~ is measured and quantified by recording the absolute maximum

1 amplitude of ground acceleration (PGA) (Chalkias et al., 2016). In this study, the PGA map of the study area was downloaded
2 from the USGS website (<https://www.usgs.gov>).
3 ~~Landslide controlling factors, i.e., (a) slope, (b) aspect, (c) elevation, (d) lithology, (e) distance from faults, (f) distance from~~
4 ~~rivers, (g) LULC, (h) NDVI, (i) PGA, as illustrated in Fig. 3, were generated as described above.~~ To ensure the consistency
5 and easy process of these data, all factor layers were converted into raster data format (GeoTIFF) with an identical spatial
6 projection (WGS84 datum) and resampled to a resolution of 30 m by ENVI 5.3 and ArcGIS 10.2.

7 **4 Methodology**

8 In this study, an integrated weighted index model was developed as a complete landslide susceptibility model by combining
9 AHP and FR approaches. ~~The assumption behind the integrated weighted index model was that future landslides will occur~~
10 ~~under similar environmental conditions as historical landslides (Guzzetti et al., 1999; Pourghasemi and Rahmati, 2018), and~~
11 ~~the susceptibility can be evaluated from the relationship between the controlling factors and the landslide occurrence area (Zhu~~
12 ~~et al., 2014).~~ In the present study, As shown in Fig. 4, the integrated weighted index model was run through three general steps:
13 (1) determining the relative importance of landslide controlling factors using AHP method, (2) characterizing the relationships
14 between controlling factors and landslide locations using FR and GIS techniques, and (3) predicting landslide susceptibility
15 using ~~weighted overlay analysis~~ Weighted Overlay Analysis tool of ArcGIS. ~~The integrated model can assess the correlation~~
16 ~~between the controlling factors and also the influence of each landslide controlling factor on landslide occurrence.~~
17 ~~The integrated weighted index was calculated as follows:~~

$$18 \quad I = \sum_i^m (W_i \times FR_i) , \quad (2)$$

19 ~~Where, m stands for number of controlling factors, W_i is the weight of each controlling factor calculated by the AHP method,~~
20 ~~FR_i is the FR value of the controlling factor calculated by the FR method.~~

21 **4.1 Analytical hierarchy process (AHP)**

22 The AHP method, developed by Saaty (Saaty, 1977), is an important multiple criteria decision-making method (Vaidya and
23 Kumar, 2006), which has been applied for landslide susceptibility assessment for many years (Akgun, 2012; Barredo et al.,
24 2000; Kayastha et al., 2013; Komac, 2006; Pourghasemi et al., 2012; Yalcin, 2008).

25 ~~For the AHP, a complex non-structural problem was broken into its component parameters which were considered as the~~
26 ~~factors of this study. Then, the contribution of factors was converted into numerical values with the help of a pair wise~~
27 ~~comparison matrix generated through comparing the relative importance of each factor based on the expert's prior experience~~
28 ~~and knowledge (Vargas, 1990). In addition, it also provided a methodology to judge the relative importance of factors by~~

~~scoring. When a factor is more important than another, the score varies between 1 and 9. Conversely, the score varies between 1/2 and 1/9. The higher the score, the greater the importance of the factor. Finally, weights of factors were determined in the process of a pair-wise comparison matrix using Python software, and the weights with the Consistency Ratio (CR) less than 0.1 were accepted.~~

In the AHP, a complex non-structural problem is first broken down into several component factors. Then, based on the expert's prior experience and knowledge, a pair-wise comparison matrix can be constructed through comparing the relative importance of each factor (Vargas, 1990). An underlying 9-point recording scale is used to rate the relative importance of factors (Mansouri Daneshvar, 2014). Specifically, when a factor is more important than another, the score varies between 1 and 9. Conversely, the score varies between 1/2 and 1/9. The higher the score, the greater the importance of the factor. With the help of a pair-wise comparison matrix, the contribution of factors can be converted into numerical values. Note that a consistency check of comparison matrix needs to be carried out, and the Consistency Ratio (CR) of less than 0.1 is generally accepted.

In this study, the relative importance of landslide controlling factors was determined from the prior experience and knowledge of experts. Since the knowledge source varies from person to person, the best judgment always comes from an individual who has good expertise (Ayalew et al., 2004). To find the appropriate correlation between controlling factors, we investigated some related literatures (Shahabi and Hashim, 2015; Xu et al., 2012b; Zhang et al., 2016) and consulted with some professional experts. Finally, the pair-wise comparison matrix was determined by means of discussion (Table 2) and a general consensus achieved by experts. Weights of factors were determined in the process of a pair-wise comparison matrix using Python software, as shown in Table 2. The Consistency Ratio (CR) for this study was 0.017, which showed that the pair-wise comparison matrix satisfied the consistency requirement.

4.2 Frequency ratio (FR)

The FR method is one of the most widely used approaches to assess the landslide susceptibility at regional scale (Guo et al., 2015; Li et al., 2017; Mohammady et al., 2012), which is based on the observed spatial relationship between landslide locations and controlling factors (Lee and Pradhan, 2007; Poudyal et al., 2010). The assumption behind the FR is that future landslides will occur under similar environmental conditions as historical landslides (Guzzetti et al., 1999; Pourghasemi and Rahmati, 2018), and the susceptibility can be evaluated from the relationship between the controlling factors and the landslide occurrence area (Zhu et al., 2014). The definition of FR is the ratio of the probability of the occurrence to the non-occurrence for given properties (Lee and Talib, 2005). The spatial relationship between landslides and controlling factors can be investigated through by using the FR method. Therefore, the FR values of each controlling factor category were calculated from their relationship with landslide occurrence locations as illustrated in Table 3. The average value of FR is 1 so that a value larger than one represents a higher correlation and those less than it, a lower correlation (Romer and Ferentinou, 2016).

1 The FR value can be calculated as follows (Ghobadi et al., 2017):

$$2 \quad FR_i = \frac{Ncell(S_i)/Ncell(N_i)}{\sum Ncell(S_i)/\sum Ncell(N_i)}, \quad (3)(2)$$

3 Where, $Ncell(S_i)$ represents number of grid cells recognized as landslides in class i , and $Ncell(N_i)$ represents total number
4 of grid cells belonging to class i in the whole area; while $\sum Ncell(S_i)$ stands for the total number of grid cells recognized as
5 landslides in the whole area, and $\sum Ncell(N_i)$ represents total number of grid cells in the whole area.

6 **4.3 Integrated weighted index**

7 The integrated weighted index is considered to measure the probability of slope failures. By combining FR and AHP methods,
8 the integrated weighted model can assess the correlation between the controlling factors and also the influence of each landslide
9 controlling factor on landslide occurrence.

10 The integrated weighted index can be calculated as follows:

$$11 \quad I = \sum_i^m (W_i \times FR_i), \quad (3)$$

12 Where, m stands for number of controlling factors, W_i is the weight of each controlling factor calculated by the AHP method,
13 FR_i is the FR value of the controlling factor calculated by the FR method.

14 In this study, the values of W_i and FR_i were used to obtain the integrated weighted index of each grid cell in the study area,
15 and the final landslide susceptibility map was generated by using Weighted Overlay Analysis tool of ArcGIS.

16 **5 Results and discussions**

17 **5.1 Landslide susceptibility mapping**

18 ~~In this study, the relative importance of landslide controlling factors was determined from the prior experience and knowledge~~
19 ~~of experts. Since the knowledge source varies from person to person, the best judgment always comes from an individual who~~
20 ~~has good expertise (Ayalew et al., 2004). To find the appropriate correlation between controlling factors, we investigated some~~
21 ~~related literatures (Shahabi and Hashim, 2015; Xu et al., 2012b; Zhang et al., 2016) and consulted with some professional~~
22 ~~experts. Finally, the pair wise comparison matrix was determined by means of discussion (Table 2) and a general consensus~~
23 ~~achieved by experts. The AHP method was used to assign the weights for each controlling factor (Table 2). The higher the~~
24 ~~weight was, the more impacts on landslide occurrence could be expected. In the As shown in Table 2, the weights for the nine~~
25 ~~controlling factors were estimated as follows: slope—0.222, aspect—0.043, elevation—0.058, lithology—0.116, distance from~~
26 ~~faults—0.197, distance from rivers—0.080, LULC—0.083, NDVI—0.043 and PGA—0.158. The Consistency Ratio was 0.017,~~
27 ~~which showed that the pair wise comparison matrix satisfied the consistency requirement. The higher the weight, the more~~

1 ~~impacts on landslide occurrence could be expected. The~~ weight of slope was highest, implying the most significant influence
2 of slope on the landslide occurrence, and the weights of aspect and NDVI were the lowest, which indicated that these two
3 factors played the least role in the landslide occurrence.

4 ~~Thus, the FR was considered as a measure for the spatial relationship between landslides and controlling factors. Through~~
5 ~~analysing the relationship between each controlling factor and the landslide occurrence, the FR values were calculated by using~~
6 ~~the Eq. (3) (as shown in Table 3). The higher the FR was, the closer the relationship between the landslide controlling factor~~
7 ~~and the landslide occurrence would be.~~ The FR values of each controlling factor category were calculated by using the Eq. (2)
8 (as shown in Table 3). Table 3 clearly shows the relationship between each controlling factor and the landslide occurrence. In
9 the term of the relationship between landslide occurrence and slope, landslides mostly occurred in the slope ranging from 40°
10 to 60°. For the elevation, landslides mostly occurred below the elevation of 3400 m, which implied that the probability of
11 landslide occurrence was higher in moderate steep mountainous region. In terms of the aspect, the FR value was very high for
12 the class of E, N, SE and NE, and it was lowest for the class of Flat. For the lithology, the highest FR value was achieved for
13 Permian System which influenced the landslide occurrence. For the factor of distance from faults, the highest FR value
14 belonged to the area higher than 2000 m. The distance from rivers with the highest FR value for frequent landslide occurrence
15 was found usually between 0 and 600 m, and landslides mostly occurred in the region with low vegetation cover of less NDVI
16 value. In the case of PGA, the value of 0.26 g had the highest FR value, which indicated the significant influence of the
17 earthquake on the landslide occurrence. In general, our results were basically consistent with the previous study (Fan et al.,
18 2018), which found that most of the landslides mainly occurred in proximity of rivers and the epicentre, with an elevation of
19 2600 m to 3200 m and a slope of 35° to 55°.

20 Finally, the ~~weighted index was calculated by using the Eq. (2). The~~ landslide susceptibility map of study area was generated
21 by using Weighted Overlay Analysis tool of ArcGIS, and the study area was classified into seven categories of landslide
22 susceptibility levels as presented in Fig. 45: very high, high, relatively high, moderate, relatively low, low and very low by
23 using Natural Breaks (Jenks) method with ArcGIS, respectively.

24 According to the landslide susceptibility map, the location close to the epicentre and rivers was classified as the most
25 susceptible areas for landslides, and the high and very high landslide susceptible areas mostly located in the middle central
26 mountainous region ~~accounting for 10.99 % of the study area.~~ The low and very low susceptibility areas far from the epicentre
27 and less affected by the earthquake, mainly distributed in the North and South-West parts of the study area, ~~accounting for~~
28 ~~approximately 35.06 % of the study area. Generally, the landslide susceptibility map generated by the integrated weighted~~
29 ~~index model can reflect the potential area of the landslide occurrence in the study area.~~ Table 4 presented the distribution of
30 seven landslide susceptibility levels. As indicated in Table 4, the very low susceptible area covered 9.72 % of the whole area,

1 whereas low, relatively low, moderate, relatively high, high and very high susceptible areas covered 25.34 %, 22.92 %, 17.76 %, 2 13.27 %, 7.97 % and 3.02% of the whole area, respectively. A total of 61.76 % of the landslides were observed in the high and 3 very high susceptibility areas, and only 3.08 % of the landslides were observed in the low and very low susceptibility areas. 4 For the landslide density, the values for very low, low, relatively low, moderate, relatively high, high and very high were 0.03, 5 0.06, 0.11, 0.37, 0.96, 3.03 and 4.79, respectively. The landslide density for the very high susceptible area was significantly 6 larger than for the other susceptible areas.

7 **5.2 Validations**

8 For landslide susceptibility mapping, ~~detailed~~ validation of the modelled results is essential. A simple procedure of validation 9 can make a comprehensive and reasonable interpretation of the future landslide hazard (Chung and Fabbri, 2003).

10 In this study, operating characteristics curve (ROC) approach (Brenning, 2005; Bui et al., 2016) was adopted to evaluate the 11 performance of the integrated weighted index model, including the degree of model fit and model predictive capability. The 12 ROC curve was obtained by calculating the area under the curve (AUC) and the AUC value varied from 0.5 to 1.0 (Umar et 13 al., 2014). The AUC value of 1.0 implied a perfect performance of the model, whereas a value close to 0.5 indicated that the 14 model performed not so well. To assess the fitting performance of the integrated weighted index model, five sub-datasets 15 containing 20 %, 40 %, 60 %, 80 % and 100 % of training dataset (i.e., 673 landslides) respectively, were used to obtain the 16 fitting curves (~~Fig. 5(a)~~). Figure 56(a) shows a quantitative measure of the ability of integrated weighted index model to 17 describe the known distribution of landslides. The AUC values of five sub-datasets were 82.57 %, 84.52 %, 84.99 %, 86.08 % 18 and 85.65 %, respectively, which suggested the effective fitting capability of the integrated weighted index model developed 19 in this study.

20 To investigate the prediction performance of the integrated weighted index model, we also adopted five sub-datasets containing 21 20 %, 40 %, 60 %, 80 % and 100 % of validation dataset (i.e., 169 landslides) respectively, to estimate the prediction rates. 22 Note that the validation dataset (i.e., 20 % of the landslide inventory dataset) was not used in the training process. The AUC 23 values of five sub-datasets, as presented in Fig. 56(b), were 78.71 %, 81.66 %, 84.27 %, 86.09 % and 87.16 %, respectively. 24 With the increase of input data, the performance of the integrated weighted index model was significantly improved, which 25 indicated a reliable predicting capability of the integrated weighted index model adopted in this study.

26 In addition, the landslide density distribution of each susceptibility level was computed by associating landslides with the 27 classified landslide susceptibility map (as shown in Table 4). There was a clear trend that the increase in the level of landslide 28 susceptibility was highly correlated with the density of landslides. The high and very high susceptibility levels had the 29 significant high landslide density values, while the low susceptibility categories were just the opposite, which also implied the 30 effectiveness of the generated landslide susceptibility map of the study area.

1 5.3 Discussions

2 Landslide susceptibility is defined as the likelihood of landslides occurring in an area under local environmental conditions
3 (Fell et al., 2008; Reichenbach et al., 2018). ~~The susceptibility can be evaluated from the relationship between the~~
4 ~~environmental conditions and previous landslides (Zhu et al., 2014). There are numerous methods that have been proposed to~~
5 ~~model this relationship.~~ There are numerous methods that have been proposed to evaluate the susceptibility. The main purpose
6 of this study ~~was~~ ~~is~~ to assess the spatial probability of landslide occurrences by using an integrated weighted index model in
7 association with the utilization of FR and AHP approaches ~~to generate an earthquake-triggered landslide susceptibility map.~~
8 ~~To achieve this objective, nine controlling factors (slope, aspect, elevation, lithology, distance from faults, and distance from~~
9 ~~rivers, LULC, NDVI and PGA) were taken into consideration.~~ The FR is a data-driven statistical approach which can derive
10 spatial relationship between landslide locations and controlling factors. However, the FR method does not consider the mutual
11 relationships between controlling factors. The AHP method is an important multiple criteria decision-making method, which
12 can overcome this shortcoming. To some extent, the integrated method preserves the advantages of FR and AHP methods and
13 restrains their weak points. Some similar studies have also pointed it out (Reichenbach et al., 2018; Youssef et al., 2015; Zhou
14 et al., 2016).

15 The implementation of the integrated weighted index model revealed that landslide susceptibility levels were basically
16 consistent with the distribution of earthquake-triggered landslides. The high susceptibility areas were concentrated in the
17 central mountainous region close to the epicentre of the earthquake of the study area, which indicated the significant influence
18 of the Jiuzhaigou earthquake on the landslide occurrence. From the landslide susceptibility map (as shown in Fig. 5 and Table
19 4), the “very high” and “high” susceptibility areas covered 10.99 % of the whole area ~~a significant part of the study area (10.99 %~~
20 ~~of the whole area)~~ and most of the Jiuzhaigou National Nature Reserve was classified as the most landslide susceptible areas.
21 Even though, some limitations yet existed in the proposed method. Firstly, the accuracy of FR method is highly depended on
22 the quality of dataset, especially the landslide inventory (Zhou et al., 2016). Nevertheless, the landslide inventory is generally
23 incomplete (Fell et al., 2008), and is affected by many factors, such as the quality and scale of remote sensing images, the
24 tectonic setting complexity of study area, and the expertise of the interpreter involved (Malamud et al., 2004). In this study,
25 we mainly focused on the interpretation of earthquake-triggered landslides, ~~and interpretation results were basically consistent~~
26 ~~with the previous studies (Fan et al., 2018; Wang et al., 2018a; Wang et al., 2018b).~~ We didn’t accurately identify the landslides
27 before the Jiuzhaigou earthquake due to the limitations of historical images, and smaller landslides were also not completely
28 identified. Future work should focus on the preparation of more detailed landslide inventories. Secondly, in this study, as the
29 proposed method was applied to medium-scale datasets, the results may not be suitable for specific analysis of large or detailed
30 scale. At large or detailed scales, more detailed landslide inventory dataset and controlling factor layers ~~were~~ ~~are~~ required.

1 Additionally, the assumption behind much of the landslide susceptibility mapping is that future landslides will occur under
2 similar environmental conditions as historical landslides (Guzzetti et al., 1999; Pourghasemi and Rahmati, 2018). However,
3 results obtained in the past environmental conditions are not a guarantee for the future (Guzzetti et al., 2005). *In this study, we*
4 *used a weighted index model by integrating the AHP and FR approaches to map the earthquake-triggered landslides*
5 *susceptibility and the generated susceptibility map of the study area was made for the present situation.* The susceptibility
6 results need to be adapted as soon as environmental conditions or their causal relationships obviously change in the future,
7 ~~such as urban sprawl (van Westen et al., 2008).~~ Despite its limitations, the integrated method can generate a reliable landslide
8 susceptibility map at regional scale which can provide the ~~scientific basis~~ *rapid assessment* for reconstruction of tourism
9 facilities, regional disaster management etc.

10 **6 Conclusions**

11 Earthquake is one of the dynamic causes in landslide occurrence. Earthquake-triggered landslides can cause extensive and
12 significant damages to both lives and properties. In this study, given the main motivation to adopt an integrated weighted index
13 model based on FR and AHP methods for earthquake-triggered landslide susceptibility mapping at the Zhangzha town of the
14 Jiuzhaigou County where a ~~Ms 7.0~~ *Mw 6.5* earthquake struck on Tuesday, 8 August 2017, nine factors such as slope, aspect,
15 elevation, lithology, distance from faults, distance from rivers, LULC, NDVI and PGA as landslide controlling factors were
16 adopted in the integrated weighted index model for generating the landslide susceptibility map of the study area with
17 reclassification of seven levels of landslide susceptibility areas within a GIS environment. The ROC approach was used to
18 comprehensively evaluate the performance of the integrated weighted index model, including the degree of model fit and
19 model predictive capability. The results demonstrated the reliability and feasibility of the integrated weighted index model in
20 landslide susceptibility mapping at regional scale.

21 Even some limitations do exist, the integrated weighted index model can generate a reliable landslide susceptibility map at
22 regional scale that is useful for ~~servicing the scientific basis for disaster mitigation and management.~~ *engineers and decision*
23 *makers to understand the probability of landslides and mitigate hazards.* Furthermore, the integration of some machine learning
24 techniques should be taken into account in the integrated weighted index model for advancement in future studies.

25 **Acknowledgments**

26 This study was supported by the National Key Research and Development Program of China, Grant No. 2016YFB0502502
27 and No. 2016YFA0602302. We would like to thank reviewers for their valuable suggestions and comments.

1 **References**

- 2 Akgun, A.: A comparison of landslide susceptibility maps produced by logistic regression, multi-criteria decision, and
3 likelihood ratio methods: a case study at İzmir, Turkey, *Landslides*, 9, 93-106, doi: 10.1007/s10346-011-0283-7, 2012.
- 4 Alexander, D. E.: A brief survey of GIS in mass-movement studies, with reflections on theory and methods, *Geomorphology*,
5 94, 261-267, doi: 10.1016/j.geomorph.2006.09.022, 2008.
- 6 Althuwaynee, O. F., Pradhan, B., and Lee, S.: Application of an evidential belief function model in landslide susceptibility
7 mapping, *Computers & Geosciences*, 44, 120-135, doi: 10.1016/j.cageo.2012.03.003, 2012.
- 8 Ayalew, L., Yamagishi, H., and Ugawa, N.: Landslide susceptibility mapping using GIS-based weighted linear combination,
9 the case in Tsugawa area of Agano River, Niigata Prefecture, Japan, *Landslides*, 1, 73-81, doi: 10.1007/s10346-003-0006-9,
10 2004.
- 11 Ayalew, L., and Yamagishi, H.: The application of GIS-based logistic regression for landslide susceptibility mapping in the
12 Kakuda-Yahiko Mountains, Central Japan, *Geomorphology*, 65, 15-31, doi: 10.1016/j.geomorph.2004.06.010, 2005.
- 13 Ba, Q., Chen, Y., Deng, S., Wu, Q., Yang, J., and Zhang, J.: An Improved Information Value Model Based on Gray Clustering
14 for Landslide Susceptibility Mapping, *ISPRS International Journal of Geo-Information*, 6, doi: 10.3390/ijgi6010018, 2017.
- 15 Bai, S.-B., Wang, J., Lü, G.-N., Zhou, P.-G., Hou, S.-S., and Xu, S.-N.: GIS-based logistic regression for landslide
16 susceptibility mapping of the Zhongxian segment in the Three Gorges area, China, *Geomorphology*, 115, 23-31, doi:
17 10.1016/j.geomorph.2009.09.025, 2010.
- 18 [Barredo, J., Benavides, A., Hervás, J., and van Westen, C. J.: Comparing heuristic landslide hazard assessment techniques
19 using GIS in the Tirajana basin, Gran Canaria Island, Spain, *International Journal of Applied Earth Observation and
20 Geoinformation*, 2, 9-23, doi: 10.1016/S0303-2434\(00\)85022-9, 2000.](#)
- 21 Boon, D. P., Chambers, J. E., Hobbs, P. R. N., Kirkham, M., Merritt, A. J., Dashwood, C., Pennington, C., and Wilby, P. R.:
22 A combined geomorphological and geophysical approach to characterising relict landslide hazard on the Jurassic Escarpments
23 of Great Britain, *Geomorphology*, 248, 296-310, doi: 10.1016/j.geomorph.2015.07.005, 2015.
- 24 Brenning, A.: Spatial prediction models for landslide hazards: review, comparison and evaluation, *Nat Hazard Earth Sys*, 5,
25 853-862, doi: 10.5194/nhess-5-853-2005, 2005.
- 26 Bui, D. T., Tuan, T. A., Klempe, H., Pradhan, B., and Revhaug, I.: Spatial prediction models for shallow landslide hazards: a
27 comparative assessment of the efficacy of support vector machines, artificial neural networks, kernel logistic regression, and
28 logistic model tree, *Landslides*, 13, 361-378, doi: 10.1007/s10346-015-0557-6, 2016.
- 29 [Caniani, D., Pascale, S., Sdao, F., and Sole, A.: Neural networks and landslide susceptibility: a case study of the urban area of
30 Potenza, *Natural Hazards*, 45, 55-72, doi: 10.1007/s11069-007-9169-3, 2008.](#)

1 Carrara, A., Cardinali, M., Detti, R., Guzzetti, F., Pasqui, V., and Reichenbach, P.: Gis Techniques and Statistical-Models in
2 Evaluating Landslide Hazard, *Earth Surf Proc Land*, 16, 427-445, doi: 10.1002/esp.3290160505, 1991.

3 [Catani, F., Casagli, N., Ermini, L., Righini, G., and Menduni, G.: Landslide hazard and risk mapping at catchment scale in the
4 Arno River basin, *Landslides*, 2, 329-342, doi: 10.1007/s10346-005-0021-0, 2005.](#)

5 Chalkias, C., Polykretis, C., Ferentinou, M., and Karymbalis, E.: Integrating Expert Knowledge with Statistical Analysis for
6 Landslide Susceptibility Assessment at Regional Scale, *Geosciences*, 6, 14, doi: 10.3390/geosciences6010014, 2016.

7 Chung, C. J. F., and Fabbri, A. G.: Validation of spatial prediction models for landslide hazard mapping, *Nat Hazards*, 30,
8 451-472, doi: 10.1023/B:Nhaz.0000007172.62651.2b, 2003.

9 Conforti, M., Pascale, S., Robustelli, G., and Sdao, F.: Evaluation of prediction capability of the artificial neural networks for
10 mapping landslide susceptibility in the Turbolo River catchment (northern Calabria, Italy), *Catena*, 113, 236-250, doi:
11 10.1016/j.catena.2013.08.006, 2014.

12 Dai, F. C., and Lee, C. F.: Landslide characteristics and, slope instability modeling using GIS, Lantau Island, Hong Kong,
13 *Geomorphology*, 42, 213-228, doi: 10.1016/S0169-555x(01)00087-3, 2002.

14 Dehnavi, A., Aghdam, I. N., Pradhan, B., and Morshed Varzandeh, M. H.: A new hybrid model using step-wise weight
15 assessment ratio analysis (SWARA) technique and adaptive neuro-fuzzy inference system (ANFIS) for regional landslide
16 hazard assessment in Iran, *Catena*, 135, 122-148, doi: 10.1016/j.catena.2015.07.020, 2015.

17 [Deng, G.: Study of Tourism Geosciences Landscape Formation and Protection of Jiuzhaigou World Natural Heritage Site,
18 Ph.D. thesis, Chengdu University of Technology, China, 173 pp., 2011 \(in Chinese\).](#)

19 [Ermini, L., Catani, F., Casagli, N.: Artificial Neural Networks applied to landslide susceptibility assessment, *Geomorphology*,
20 66, 327-343, doi: 10.1016/j.geomorph.2004.09.025, 2005.](#)

21 Fan, X., Scaringi, G., Xu, Q., Zhan, W., Dai, L., Li, Y., Pei, X., Yang, Q., and Huang, R.: Coseismic landslides triggered by
22 the 8th August 2017 Ms 7.0 Jiuzhaigou earthquake (Sichuan, China): factors controlling their spatial distribution and
23 implications for the seismogenic blind fault identification, *Landslides*, 15, 967-983, doi: 10.1007/s10346-018-0960-x, 2018.

24 Fell, R., Corominas, J., Bonnard, C., Cascini, L., Leroi, E., and Savage, W. Z.: Guidelines for landslide susceptibility, hazard
25 and risk zoning for land use planning, *Engineering Geology*, 102, 85-98, doi: 10.1016/j.enggeo.2008.03.022, 2008.

26 [Florsheim, J.L., Ustin, S.L., Tang, Y., Di, B., Huang, C., Qiao, X., Peng, H., Zhang, M., Cai, Y.: Basin-scale and travertine
27 dam-scale controls on fluvial travertine, Jiuzhaigou, southwestern China, *Geomorphology*, 180-181, 267-280, doi:
28 10.1016/j.geomorph.2012.10.016, 2013.](#)

1 Ghobadi, M. H., Nouri, M., Saedi, B., Jalali, S. H., and Pirouzinajad, N.: The performance evaluation of information value,
2 density area, LNRF, and frequency ratio methods for landslide zonation at Miandarband area, Kermanshah Province, Iran,
3 *Arabian Journal of Geosciences*, 10, doi: 10.1007/s12517-017-3202-y, 2017.

4 Guo, C., Montgomery, D. R., Zhang, Y., Wang, K., and Yang, Z.: Quantitative assessment of landslide susceptibility along
5 the Xianshuihe fault zone, Tibetan Plateau, China, *Geomorphology*, 248, 93-110, doi: 10.1016/j.geomorph.2015.07.012, 2015.

6 Guzzetti, F., Carrara, A., Cardinali, M., and Reichenbach, P.: Landslide hazard evaluation: a review of current techniques and
7 their application in a multi-scale study, Central Italy, *Geomorphology*, 31, 181-216, doi: 10.1016/S0169-555x(99)00078-1,
8 1999.

9 Guzzetti, F., Reichenbach, P., Cardinali, M., Galli, M., and Ardizzone, F.: Probabilistic landslide hazard assessment at the
10 basin scale, *Geomorphology*, 72, 272-299, doi: 10.1016/j.geomorph.2005.06.002, 2005.

11 Guzzetti, F., Mondini, A. C., Cardinali, M., Fiorucci, F., Santangelo, M., and Chang, K. T.: Landslide inventory maps: New
12 tools for an old problem, *Earth-Sci Rev*, 112, 42-66, doi: 10.1016/j.earscirev.2012.02.001, 2012.

13 Kadavi, P., Lee, C.-W., and Lee, S.: Application of Ensemble-Based Machine Learning Models to Landslide Susceptibility
14 Mapping, *Remote Sensing*, 10, doi: 10.3390/rs10081252, 2018.

15 [Kanungo, D.P.; Arora, M.K.; Sarkar, S.; Gupta, R.P.: A comparative study of conventional, ANN black box, fuzzy and
16 combined neural and fuzzy weighting procedures for landslide susceptibility zonation in Darjeeling Himalayas, *Engineering
17 Geology*, 85, 347-366, doi: 10.1016/j.enggeo.2006.03.004, 2006.](#)

18 Kayastha, P., Dhital, M. R., and De Smedt, F.: Application of the analytical hierarchy process (AHP) for landslide susceptibility
19 mapping: A case study from the Tinau watershed, west Nepal, *Computers & Geosciences*, 52, 398-408, doi:
20 10.1016/j.cageo.2012.11.003, 2013.

21 Komac, M.: A landslide susceptibility model using the Analytical Hierarchy Process method and multivariate statistics in
22 perialpine Slovenia, *Geomorphology*, 74, 17-28, doi: 10.1016/j.geomorph.2005.07.005, 2006.

23 Lee, S., and Min, K.: Statistical analysis of landslide susceptibility at Yongin, Korea, *Environmental Geology*, 40, 1095-1113,
24 doi: 10.1007/s002540100310, 2001.

25 [Lee, S., and Pradhan, B.: Landslide hazard mapping at Selangor, Malaysia using frequency ratio and logistic regression models,
26 *Landslides*, 4, 33-41, doi: 10.1007/s10346-006-0047-y, 2007.](#)

27 Lee, S.: Application of logistic regression model and its validation for landslide susceptibility mapping using GIS and remote
28 sensing data, *International Journal of Remote Sensing*, 26, 1477-1491, doi: 10.1080/01431160412331331012, 2005.

29 Lee, S., and Talib, J. A.: Probabilistic landslide susceptibility and factor effect analysis, *Environmental Geology*, 47, 982-990,
30 doi: 10.1007/s00254-005-1228-z, 2005.

1 Lei, H., Wang, X., Hou, H., Su, L., Yu, D., and Wang, H.: The earthquake in Jiuzhaigou County of Northern Sichuan, China
2 on August 8, 2017, *Natural Hazards*, 90, 1021-1030, doi: 10.1007/s11069-017-3064-3, 2018.

3 Li, L., Lan, H., Guo, C., Zhang, Y., Li, Q., and Wu, Y.: A modified frequency ratio method for landslide susceptibility
4 assessment, *Landslides*, 14, 727-741, doi: 10.1007/s10346-016-0771-x, 2017.

5 Li, S., Hu, X., Tang, Y., Huang, C., and Xiao, W.: Changes in lacustrine environment due to anthropogenic activities over 240
6 years in Jiuzhaigou National Nature Reserve, southwest China, *Quaternary International*, 349, 367-375, doi:
7 10.1016/j.quaint.2014.07.069, 2014.

8 Malamud, B. D., Turcotte, D. L., Guzzetti, F., and Reichenbach, P.: Landslide inventories and their statistical properties, *Earth
9 Surf Proc Land*, 29, 687-711, doi: 10.1002/esq.1064, 2004.

10 Mansouri Daneshvar, M. R.: Landslide susceptibility zonation using analytical hierarchy process and GIS for the Bojnurd
11 region, northeast of Iran, *Landslides*, 11, 1079-1091, doi: 10.1007/s10346-013-0458-5, 2014.

12 Mantovani, F., Soeters, R., and VanWesten, C. J.: Remote sensing techniques for landslide studies and hazard zonation in
13 Europe, *Geomorphology*, 15, 213-225, doi: 10.1016/0169-555x(95)00071-C, 1996.

14 [Manzo, G., Tofani, V., Segoni, S., Battistini, A., and Catani, F.: GIS techniques for regional-scale landslide susceptibility
15 assessment: the Sicily \(Italy\) case study, *International Journal of Geographical Information Science*, 27, 1433-1452, doi:
16 10.1080/13658816.2012.693614, 2013.](#)

17 Marjanović, M., Kovačević, M., Bajat, B., and Voženilek, V.: Landslide susceptibility assessment using SVM machine
18 learning algorithm, *Engineering Geology*, 123, 225-234, doi: 10.1016/j.enggeo.2011.09.006, 2011.

19 Mohammady, M., Pourghasemi, H. R., and Pradhan, B.: Landslide susceptibility mapping at Golestan Province, Iran: A
20 comparison between frequency ratio, Dempster–Shafer, and weights-of-evidence models, *Journal of Asian Earth Sciences*, 61,
21 221-236, doi: 10.1016/j.jseaes.2012.10.005, 2012.

22 Nefeslioglu, H. A., Sezer, E., Gokceoglu, C., Bozkir, A. S., and Duman, T. Y.: Assessment of Landslide Susceptibility by
23 Decision Trees in the Metropolitan Area of Istanbul, Turkey, *Mathematical Problems in Engineering*, 2010, 1-15, doi:
24 10.1155/2010/901095, 2010.

25 Ozdemir, A., and Altural, T.: A comparative study of frequency ratio, weights of evidence and logistic regression methods for
26 landslide susceptibility mapping: Sultan Mountains, SW Turkey, *Journal of Asian Earth Sciences*, 64, 180-197, doi:
27 10.1016/j.jseaes.2012.12.014, 2013.

28 Pellicani, R., and Spilotro, G.: Evaluating the quality of landslide inventory maps: comparison between archive and surveyed
29 inventories for the Daunia region (Apulia, Southern Italy), *B Eng Geol Environ*, 74, 357-367, doi: 10.1007/s10064-014-0639-
30 z, 2015.

1 Peng, L., Niu, R., Huang, B., Wu, X., Zhao, Y., and Ye, R.: Landslide susceptibility mapping based on rough set theory and
2 support vector machines: A case of the Three Gorges area, China, *Geomorphology*, 204, 287-301, doi:
3 10.1016/j.geomorph.2013.08.013, 2014.

4 Pham, B. T., Prakash, I., and Bui, D. T.: Spatial prediction of landslides using a hybrid machine learning approach based on
5 Random Subspace and Classification and Regression Trees, *Geomorphology*, 303, 256-270, doi:
6 10.1016/j.geomorph.2017.12.008, 2018.

7 Poudyal, C. P., Chang, C., Oh, H.-J., and Lee, S.: Landslide susceptibility maps comparing frequency ratio and artificial neural
8 networks: a case study from the Nepal Himalaya, *Environmental Earth Sciences*, 61, 1049-1064, doi: 10.1007/s12665-009-
9 0426-5, 2010.

10 Pourghasemi, H. R., Pradhan, B., and Gokceoglu, C.: Application of fuzzy logic and analytical hierarchy process (AHP) to
11 landslide susceptibility mapping at Haraz watershed, Iran, *Nat Hazards*, 63, 965-996, doi: 10.1007/s11069-012-0217-2, 2012.

12 Pourghasemi, H. R., and Rahmati, O.: Prediction of the landslide susceptibility: Which algorithm, which precision?, *Catena*,
13 162, 177-192, doi: 10.1016/j.catena.2017.11.022, 2018.

14 Pradhan, B., and Lee, S.: Regional landslide susceptibility analysis using back-propagation neural network model at Cameron
15 Highland, Malaysia, *Landslides*, 7, 13-30, doi: 10.1007/s10346-009-0183-2, 2009.

16 Regmi, N. R., Giardino, J. R., and Vitek, J. D.: Modeling susceptibility to landslides using the weight of evidence approach:
17 Western Colorado, USA, *Geomorphology*, 115, 172-187, doi: 10.1016/j.geomorph.2009.10.002, 2010.

18 Reichenbach, P., Rossi, M., Malamud, B. D., Mihir, M., and Guzzetti, F.: A review of statistically-based landslide
19 susceptibility models, *Earth-Sci Rev*, 180, 60-91, doi: 10.1016/j.earscirev.2018.03.001, 2018.

20 Romer, C., and Ferentinou, M.: Shallow landslide susceptibility assessment in a semiarid environment — A Quaternary
21 catchment of KwaZulu-Natal, South Africa, *Engineering Geology*, 201, 29-44, doi: 10.1016/j.enggeo.2015.12.013, 2016.

22 Saaty, T. L.: A scaling method for priorities in hierarchical structures, *Journal of Mathematical Psychology*, 15, 234-281, doi:
23 10.1016/0022-2496(77)90033-5, 1977.

24 Saha, A. K., Gupta, R. P., and Arora, M. K.: GIS-based Landslide Hazard Zonation in the Bhagirathi (Ganga) Valley,
25 Himalayas, *International Journal of Remote Sensing*, 23, 357-369, doi: 10.1080/01431160010014260, ~~2010~~2002.

26 Saito, H., Nakayama, D., and Matsuyama, H.: Comparison of landslide susceptibility based on a decision-tree model and actual
27 landslide occurrence: The Akaiishi Mountains, Japan, *Geomorphology*, 109, 108-121, doi: 10.1016/j.geomorph.2009.02.026,
28 2009.

1 Sato, H. P., Hasegawa, H., Fujiwara, S., Tobita, M., Koarai, M., Une, H., and Iwahashi, J.: Interpretation of landslide
2 distribution triggered by the 2005 Northern Pakistan earthquake using SPOT 5 imagery, *Landslides*, 4, 113-122, doi:
3 10.1007/s10346-006-0069-5, 2007.

4 Shahabi, H., and Hashim, M.: Landslide susceptibility mapping using GIS-based statistical models and Remote sensing data
5 in tropical environment, *Scientific Reports*, 5, 9899, doi: 10.1038/srep09899, 2015.

6 Shrestha, S., Kang, T.-S., and Suwal, M.: An Ensemble Model for Co-Seismic Landslide Susceptibility Using GIS and Random
7 Forest Method, *ISPRS International Journal of Geo-Information*, 6, 365, doi: 10.3390/Ijgi6110365, 2017.

8 Siqueira, D. S., Marques, J., Pereira, G. T., Teixeira, D. B., Vasconcelos, V., Carvalho Júnior, O. A., and Martins, E. S.:
9 Detailed mapping unit design based on soil–landscape relation and spatial variability of magnetic susceptibility and soil color,
10 *Catena*, 135, 149-162, doi: 10.1016/j.catena.2015.07.010, 2015.

11 [Song, Y., Gong, J., Gao, S., Wang, D., Cui, T., Li, Y., Wei, B.: Susceptibility assessment of earthquake-induced landslides
12 using Bayesian network: A case study in Beichuan, China, *Computers & Geosciences*, 42, 189-199, doi:
13 10.1016/j.cageo.2011.09.011, 2012.](#)

14 Su, C., Wang, L., Wang, X., Huang, Z., and Zhang, X.: Mapping of rainfall-induced landslide susceptibility in Wencheng,
15 China, using support vector machine, *Nat Hazards*, 76, 1759-1779, doi: 10.1007/s11069-014-1562-0, 2015.

16 Tien Bui, D., Pradhan, B., Lofman, O., Revhaug, I., and Dick, O. B.: Landslide susceptibility assessment in the Hoa Binh
17 province of Vietnam: A comparison of the Levenberg–Marquardt and Bayesian regularized neural networks, *Geomorphology*,
18 171-172, 12-29, doi: 10.1016/j.geomorph.2012.04.023, 2012.

19 Tilmant, A., Vanclooster, M., Duckstein, L., and Persoons, E.: Comparison of fuzzy and nonfuzzy optimal reservoir operating
20 policies, *J Water Res Pl-Asce*, 128, 390-398, doi: 10.1061/(Asce)0733-9496(2002)128:6(390), 2002.

21 Umar, Z., Pradhan, B., Ahmad, A., Jebur, M. N., and Tehrany, M. S.: Earthquake induced landslide susceptibility mapping
22 using an integrated ensemble frequency ratio and logistic regression models in West Sumatera Province, Indonesia, *Catena*,
23 118, 124-135, doi: 10.1016/j.catena.2014.02.005, 2014.

24 Vaidya, O. S., and Kumar, S.: Analytic hierarchy process: An overview of applications, *European Journal of Operational
25 Research*, 169, 1-29, doi: 10.1016/j.ejor.2004.04.028, 2006.

26 ~~van Westen, C. J., Castellanos, E., and Kuriakose, S. L.: Spatial data for landslide susceptibility, hazard, and vulnerability
27 assessment: An overview, *Engineering Geology*, 102, 112-131, doi: 10.1016/j.enggeo.2008.03.010, 2008.~~

28 Vargas, L. G.: An overview of the analytic hierarchy process and its applications, *European Journal of Operational Research*,
29 48, 2-8, doi: 10.1016/0377-2217(90)90056-H, 1990.

1 Wang, J., Jin, W., Cui, Y.-f., Zhang, W.-f., Wu, C.-h., and Alessandro, P.: Earthquake-triggered landslides affecting a
2 UNESCO Natural Site: the 2017 Jiuzhaigou Earthquake in the World National Park, China, *Journal of Mountain Science*, 15,
3 1412-1428, doi: 10.1007/s11629-018-4823-7, 2018a.

4 Wang, W., Chen, H., Xu, A. H., and Qu, M. H.: Analysis of the disaster characteristics and emergency response of the
5 Jiuzhaigou earthquake, *Nat Hazard Earth Sys*, 18, 1771-1783, doi: 10.5194/nhess-18-1771-2018, 2018b.

6 Xu, C., Dai, F. C., Xu, X. W., and Lee, Y. H.: GIS-based support vector machine modeling of earthquake-triggered landslide
7 susceptibility in the Jianjiang River watershed, China, *Geomorphology*, 145, 70-80, doi: 10.1016/j.geomorph.2011.12.040,
8 2012a.

9 Xu, C., Xu, X. W., Dai, F. C., and Saraf, A. K.: Comparison of different models for susceptibility mapping of earthquake
10 triggered landslides related with the 2008 Wenchuan earthquake in China, *Computers & Geosciences*, 46, 317-329, doi:
11 10.1016/j.cageo.2012.01.002, 2012b.

12 Yalcin, A.: GIS-based landslide susceptibility mapping using analytical hierarchy process and bivariate statistics in Ardesen
13 (Turkey): Comparisons of results and confirmations, *Catena*, 72, 1-12, doi: 10.1016/j.catena.2007.01.003, 2008.

14 Youssef, A. M., Pradhan, B., Jebur, M. N., and El-Harbi, H. M.: Landslide susceptibility mapping using ensemble bivariate
15 and multivariate statistical models in Fayfa area, Saudi Arabia, *Environmental Earth Sciences*, 73, 3745-3761, doi:
16 10.1007/s12665-014-3661-3, 2015.

17 Zhang, G., Cai, Y., Zheng, Z., Zhen, J., Liu, Y., and Huang, K.: Integration of the Statistical Index Method and the Analytic
18 Hierarchy Process technique for the assessment of landslide susceptibility in Huizhou, China, *Catena*, 142, 233-244, doi:
19 10.1016/j.catena.2016.03.028, 2016.

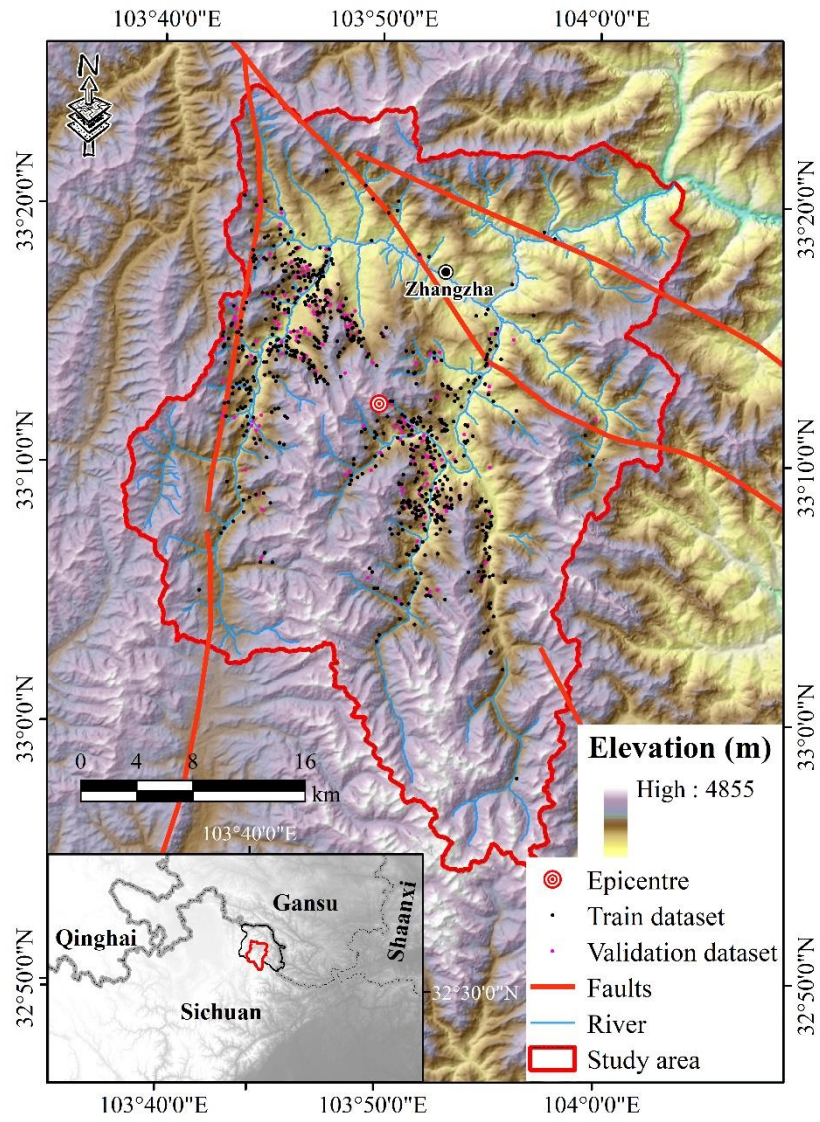
20 Zhao, B., Wang, Y.-s., Luo, Y.-h., Li, J., Zhang, X., and Shen, T.: Landslides and dam damage resulting from the Jiuzhaigou
21 earthquake (8 August 2017), Sichuan, China, *Royal Society Open Science*, 5, 171418, doi: 10.1098/rsos.171418, 2018.

22 Zhou, S. H., Chen, G. Q., Fang, L. G., and Nie, Y. W.: GIS-Based Integration of Subjective and Objective Weighting Methods
23 for Regional Landslides Susceptibility Mapping, *Sustainability*, 8, 334, doi: 10.3390/Su8040334, 2016.

24 Zhu, A. X., Wang, R. X., Qiao, J. P., Qin, C. Z., Chen, Y. B., Liu, J., Du, F., Lin, Y., and Zhu, T. X.: An expert knowledge-
25 based approach to landslide susceptibility mapping using GIS and fuzzy logic, *Geomorphology*, 214, 128-138, doi:
26 10.1016/j.geomorph.2014.02.003, 2014.

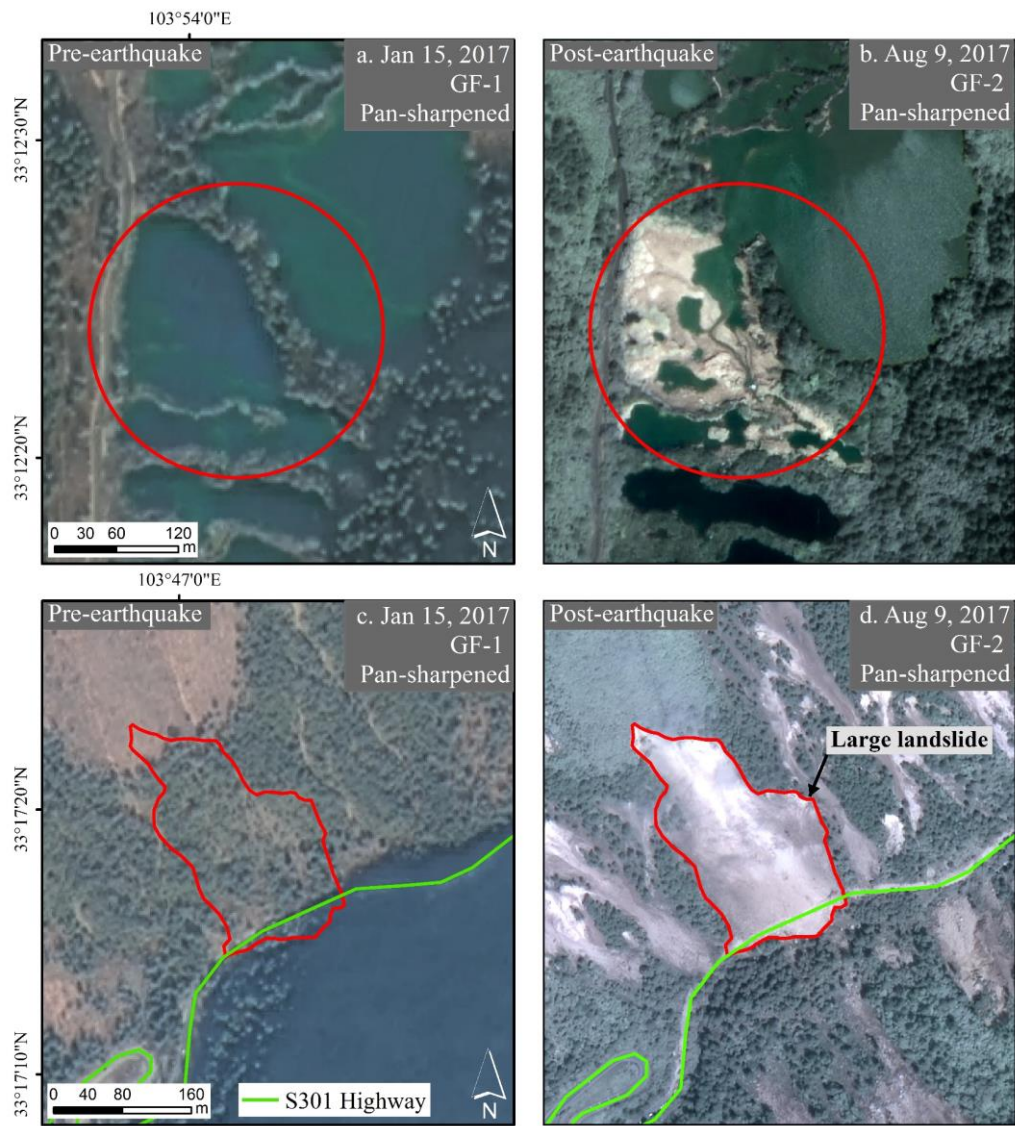
27

1 Figures



2

3 Figure 1: The digital map showing the location, topography, river networks, faults, epicentre of the Jiuzhaigou earthquake, as well
4 as the locations of earthquake-triggered landslides for training and validation over the study area.



1

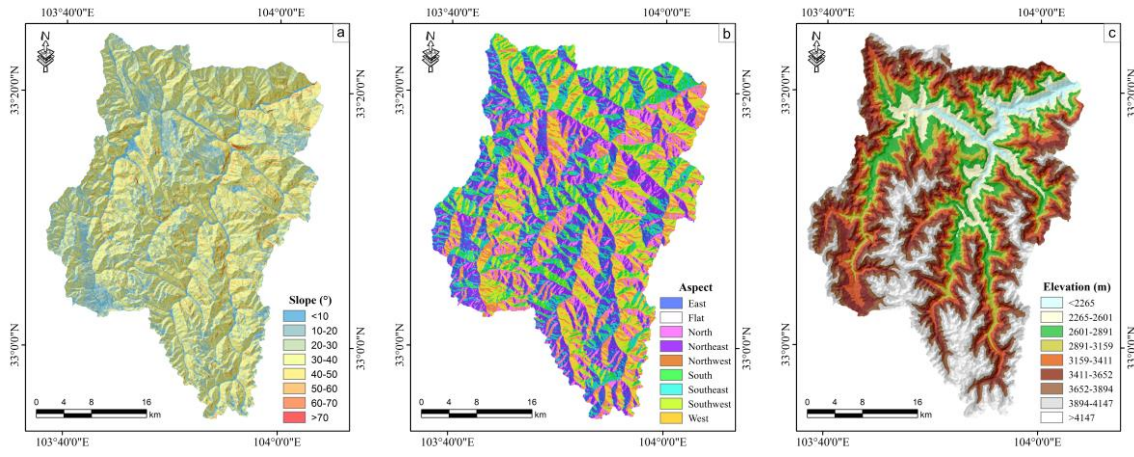
2 **Figure 2: Remote sensing interpretation for earthquake disaster of the study area. a) 2 m spatial resolution GF-1 remotely sensed**
 3 **image *acquired* on January 15, 2017 before the earthquake compared with b) 1 m spatial resolution GF-2 remotely sensed image**
 4 ***acquired* on August 9, 2017 after the earthquake, clearly revealed the dried up of the Sparkling Lake after the Jiuzhaigou earthquake;**
 5 **c) 2 m spatial resolution GF-1 remotely sensed image *acquired* on January 15, 2017 before the earthquake compared with d) 1 m**
 6 **spatial resolution GF-2 remotely sensed image *acquired* on August 9, 2017 after the earthquake, illustrated the damage of the S301**
 7 **highway in the Jiuzhaigou earthquake.**

8

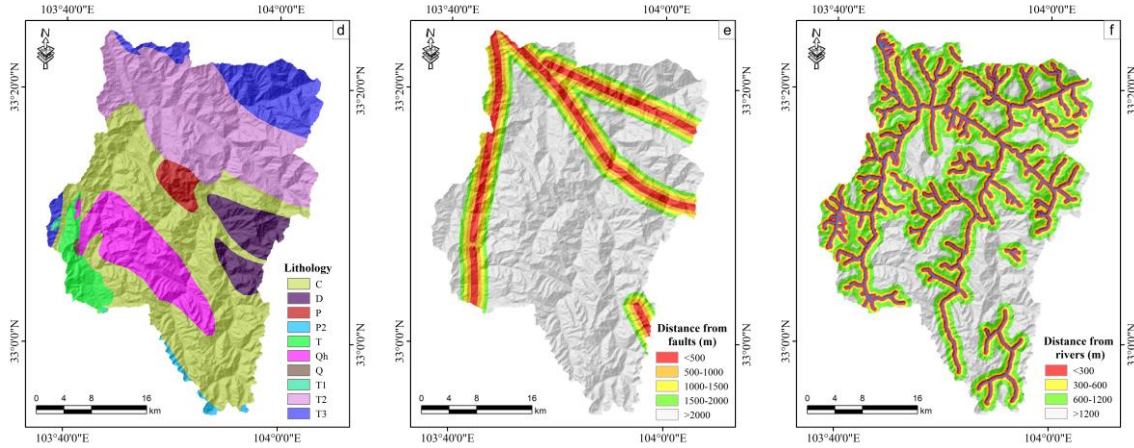
9

10

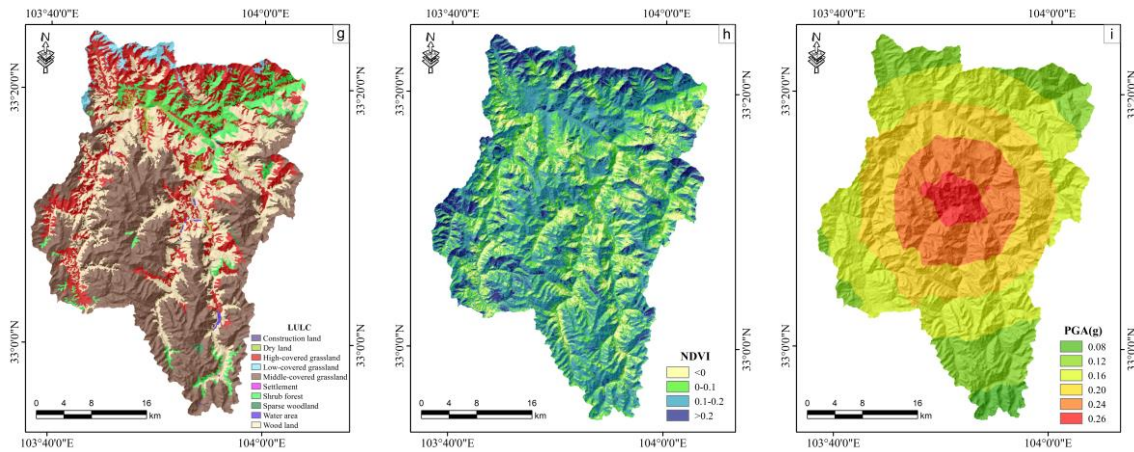
1



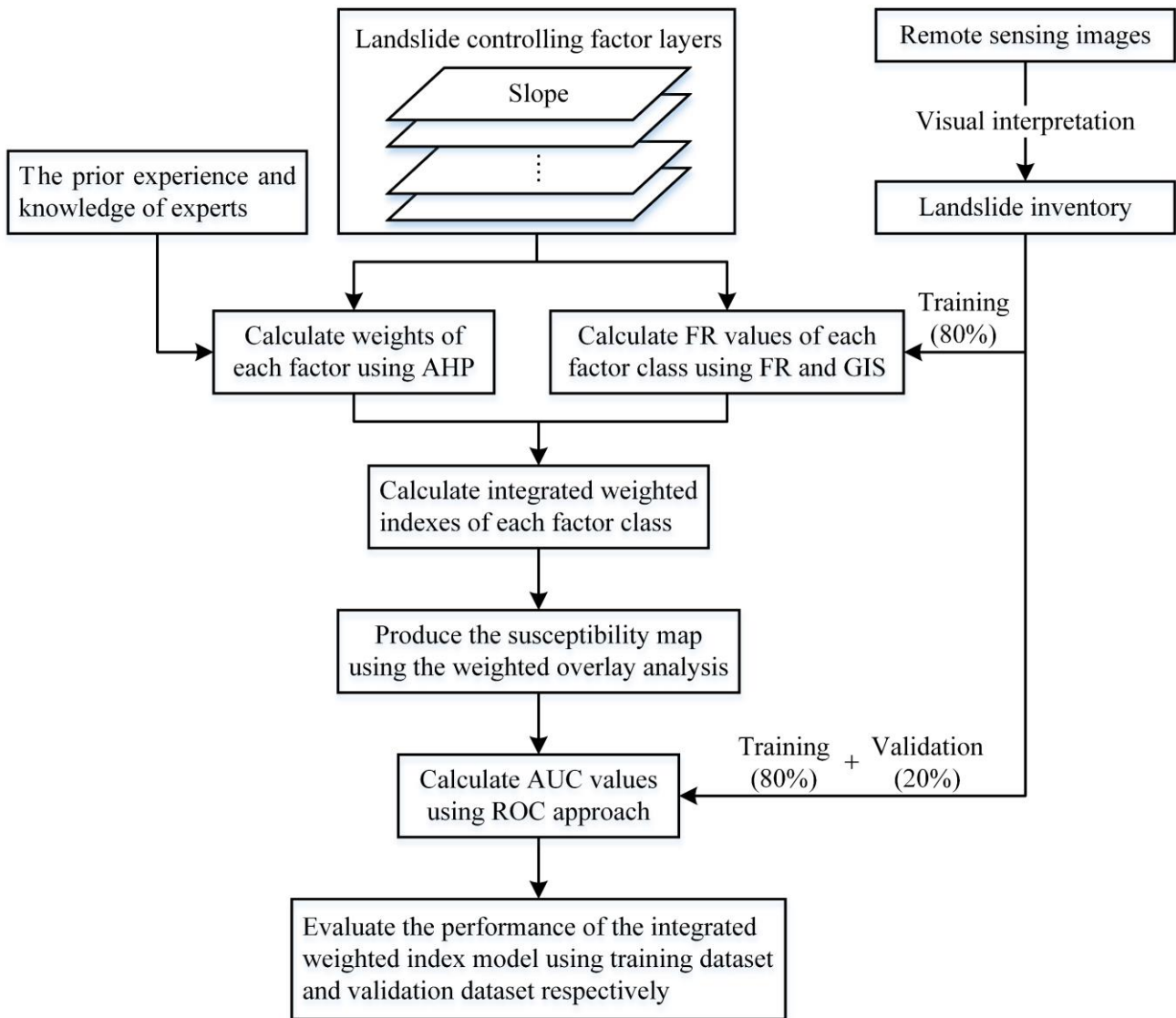
2



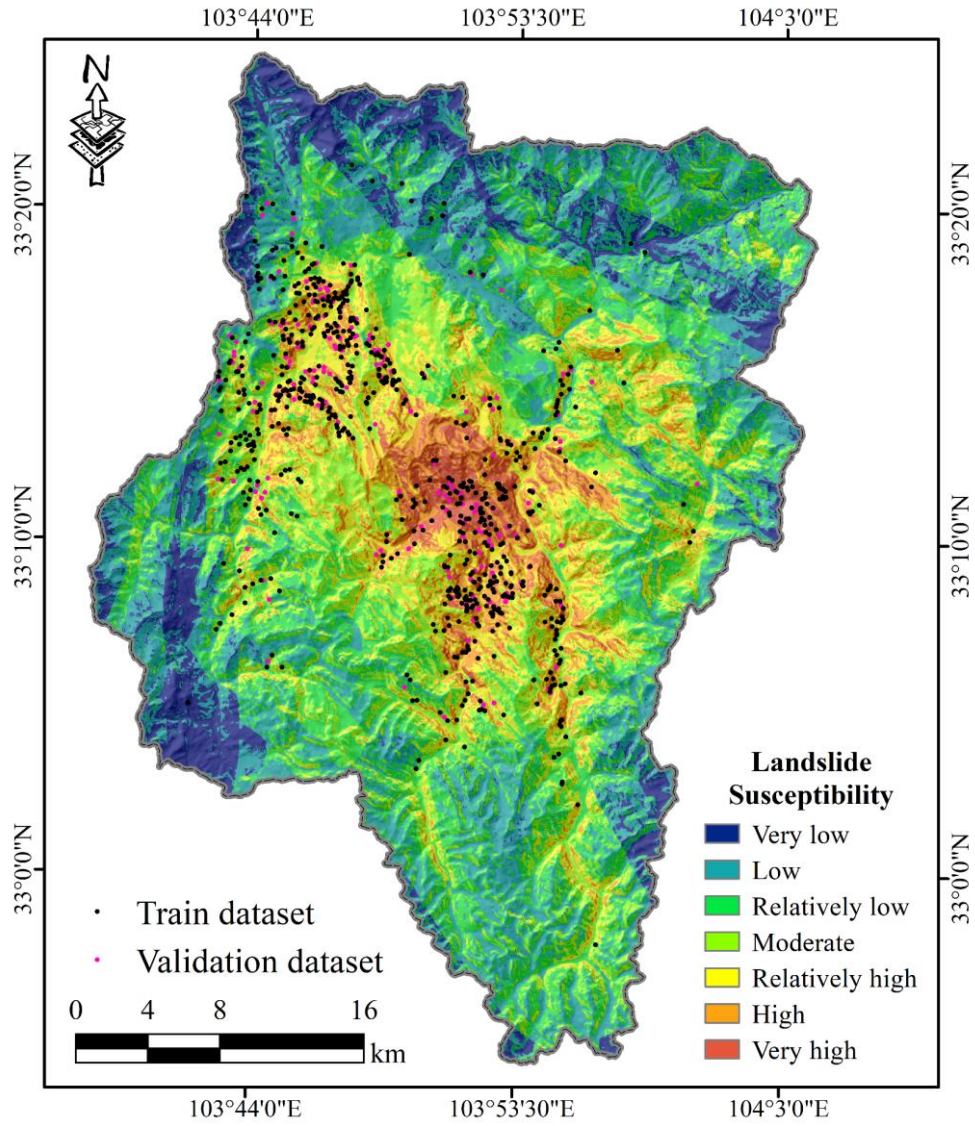
3



4 **Figure 3: Landslide controlling factor layers used for landslide susceptibility mapping in the study area. (a) Slope, (b) Aspect, (c)**
 5 **Elevation, were all extracted from DEM data, (d) Lithology, digitized from the geological map at 1: 500,000 scale, (e) Distance from**
 6 **faults, calculated by ArcGIS 10.2 software, (f) Distance from rivers, calculated by ArcGIS 10.2 software, (g) LULC, collected from**
 7 **the Geographical Information Monitoring Cloud Platform, (h) NDVI, extracted from the Landsat-8 image, (i) PGA, downloaded**
 8 **from the USGS website.**



1
2 **Figure 4: Flow chart of the landslide susceptibility mapping.**

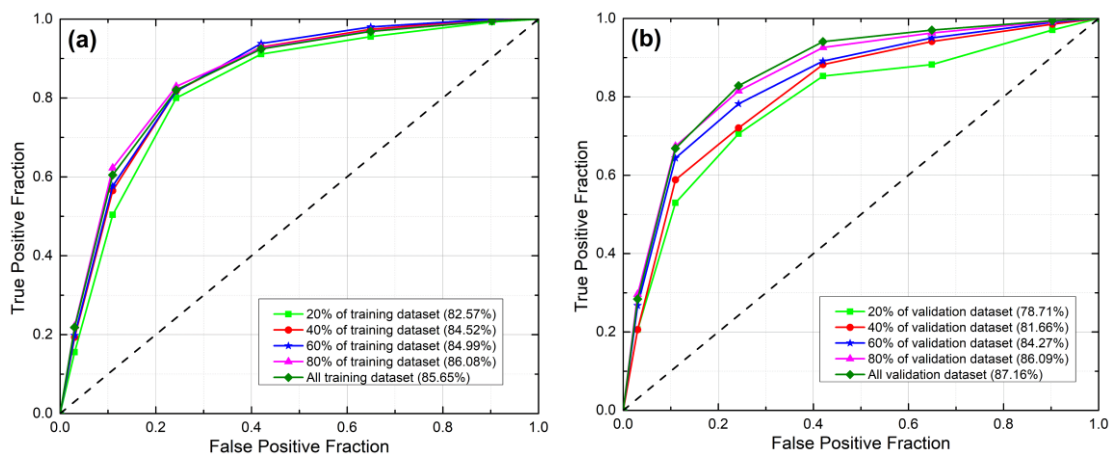


1

2

Figure 45: Landslide susceptibility map of the study area generated by using the integrated weighted index model.

3



4

5

Figure 56: ROC curves of the Jiuzhaigou landslide susceptibility assessment. (a) Fitting performance of the integrated weighted index model; (b) Prediction performance of the integrated weighted index model.

6

7

8

1 **Tables**

2 **Table 1: Data layers of the study area.**

Data layer	Data format	Scale/resolution	Data source
DEM	Grid	30 m	Shuttle Radar Topography Mission (SRTM)
Sentinel-2A	IMAGINE image	10 m	European Space Agency
Landsat-8	IMAGINE image	30 m	United States Geological Survey (USGS)
GF-1/2	IMAGINE image	2 m/1 m	China Centre for Resources Satellite Data and Application
Lithology	Shapefile (polygon)	1:500,000	The geological map
Fault	Shapefile (line)	1: 500,000	China Earthquake Administration
River	Shapefile (line)	1:10,000	Remote sensing interpretation
LULC	Grid	30 m	Geographical Information Monitoring Cloud Platform
PGA	Shapefile (polygon)	1:25,000	United States Geological Survey (USGS)

3

4

5

6 **Table 2: The pair-wise comparison matrix, factor weights, and consistency ratio obtained in present study.**

Factor	a ₁	a ₂	a ₃	a ₄	a ₅	a ₆	a ₇	a ₈	a ₉	Weight
Elevation (a ₁)	1	1/4	2	1/3	1/4	1	1/3	1/2	2	0.058
Slope (a ₂)		1	4	2	1	3	2	3	4	0.222
Aspect (a ₃)			1	1/3	1/4	1/2	1/3	1/2	1	0.043
Lithology (a ₄)				1	1/2	1	1/2	2	3	0.116
Distance from faults (a ₅)					1	2	1	3	4	0.197
LULC (a ₆)						1	1/2	1	2	0.083
PGA (a ₇)							1	2	3	0.158
Distance from rivers (a ₈)								1	2	0.080
NDVI (a ₉)									1	0.043
Consistency Ratio: 0.017										

7

8

1 **Table 3: The FR and weights for landslide controlling factors for the study area.**

Factor	Class	FR	Weight	Factor	Class	FR	Weight
Slope (°)	<10	0.000	0.222	Elevation(m)	<2265	0.451	0.058
	10-20	0.106			2265-2601	1.153	
	20-30	0.431			2601-2891	2.411	
	30-40	1.270			2891-3159	2.437	
	40-50	2.330			3159-3411	1.496	
	50-60	2.807			3411-3652	0.819	
	60-70	1.804			3652-3894	0.177	
	>70	0.000			3894-4147	0.021	
Aspect	Flat	0.000	0.043	Lithology	>4147	0.000	0.116
	N	1.305			T3	0.030	
	NE	1.116			T2	0.528	
	E	1.662			P	3.431	
	SE	1.343			C	1.819	
	SE	0.965			D	0.544	
	SW	0.590			P2	0.000	
	W	0.646			T	0.039	
	NW	0.560			T1	0.000	
	N	0.819			Qh	0.471	
Distance from faults (m)	<500	0.689	0.197	Distance from rivers (m)	Q	0.000	0.080
	500-1000	0.482			<300	1.302	
	1000-1500	0.594			300-600	1.162	
	1500-2000	0.606			600-1200	0.795	
NDVI	>2000	1.169	0.043	LULC	>1200	0.863	0.083
	<0	1.211			Dry land	0.796	
	0-0.1	1.199			Wood land	2.085	
	0.1-0.2	0.975			Shrub forest	0.164	
	>0.2	0.306			Sparse woodland	0.000	
PGA (g)	0.08	0.000	0.158		Water area	0.970	
	0.12	0.009			High-covered grassland	1.072	
	0.16	0.273			Medium-covered grassland	0.550	
	0.20	1.448			Low-covered grassland	0.000	
	0.24	2.194			Settlement	0.000	
	0.26	3.578			Construction	0.000	

2
3

1 **Table 4: Landslide susceptibility levels and density of landslides in the study area.**

Susceptibility level	Area (km ²)	Percentage of area	Number of landslide occurrences	Percentage of number	Density (no./km ²)
Very Low	130.81	9.72 %	4	0.47 %	0.03
Low	340.86	25.34 %	22	2.61 %	0.06
Relatively low	308.29	22.92 %	35	4.16 %	0.11
Moderate	238.84	17.76 %	89	10.57 %	0.37
Relatively high	178.52	13.27 %	172	20.43 %	0.96
High	107.20	7.97 %	325	38.60 %	3.03
Very High	40.67	3.02 %	195	23.16 %	4.79
Total	1345.19	100 %	842	100 %	--

2

3